Calcified Tissue International (2025) 116:30
https://doi.org/10.1007/s00223-024-01326-w

ORIGINAL RESEARCH

Administration of Bisphosphonate Preparations to Mice with Mild-type Hypophosphatasia Reduces the Quality of Spontaneous Locomotor Activity

Aki Nakamura-Takahashi[1,2] · Satoshi Ishizuka[1] · Kengo Hirai[3] · Satoru Matsunaga[2,4] · Norio Kasahara[2,5] · Seikou Shintani[2,3] · Shinichi Abe[2,4] · Masataka Kasahara[1,2]

Received: 11 June 2024 / Accepted: 4 October 2024

Abstract

Hypophosphatasia (HPP) is a congenital bone disease caused by tissue-nonspecific mutations in the alkaline phosphatase gene. It is classified into six types: severe perinatal, benign prenatal, infantile, pediatric, adult, and odonto. HPP with femoral hypoplasia on fetal ultrasonography, seizures, or early loss of primary teeth can be easily diagnosed. In contrast, pediatric, adult, and odonto types of HPP over 4 years of age are less likely to be diagnosed because they do not have typical symptoms. Consequently, it may be misdiagnosed as common osteoporosis, and treatments incompatible with HPP may be implemented. The purpose of this study was to analyze the effects of bisphosphonate preparations administration on the femur of *Akp2*$^{+/-}$ mice, a mild-type HPP mice model. Zoledronic acid (Zol) was subcutaneously administered to 4-week-old *Akp2*$^{+/-}$ mice at 1 mg/kg (volume: 200 µL) once a week for a total of 5 times. Afterward, spontaneous locomotor activity analysis was performed, and serum and femur bones were collected at 9 weeks of age. Additionally, micro-computed tomography (CT) analysis, histological analysis, and analysis of the expression levels of various marker proteins and genes were performed. Age-matched *Akp2*$^{+/+}$ mice served as controls. The results demonstrated that the administration of Zol to *Akp2*$^{+/-}$ mice, compared to *Akp2*$^{+/+}$ mice, insufficiently promotive bone formation, torn femoral head cartilage, and decreased spontaneous locomotor activity. Therefore, it is important to accurately diagnose patients with mild-type HPP.

Keywords Hypophosphatasia · Femoral head cartilage · Bone structure · Bisphosphonate · Locomotor activity

Introduction

Hypophosphatasia (HPP) is a congenital bone disease caused by decreased alkaline phosphatase (ALP) activity owing to mutations in the tissue-nonspecific alkaline phosphatase gene (*Alpl*) [1]. It is classified into six types depending on the appearance of symptoms and age: severe perinatal, benign perinatal, infantile, childhood, adult, and odonto [2]. The diagnosis of HPP is triggered by typical symptoms such as femur hypoplasia on fetal ultrasound, growth failure, epileptic seizures, or premature loss of deciduous teeth and is finally confirmed through genetic testing for *Alpl* [3]. However, patients with mild-type HPP, such as childhood, adult, and odonto HPP, who do not develop typical symptoms are often misdiagnosed with common osteoporosis, rheumatoid arthritis, or periodontal disease [4–6].

For instance, at a rheumatology outpatient clinic in Vienna, genetic testing was performed in 23 patients suspected of having HPP based on low serum ALP activity and

✉ Aki Nakamura-Takahashi
atakahashi@tdc.ac.jp

✉ Masataka Kasahara
mkasahar@tdc.ac.jp

1 Department of Pharmacology, Tokyo Dental College, 2-9-18, Kandamisaki-cho, Chiyoda-ku, Tokyo 101-0061, Japan

2 Tokyo Dental College Research Branding Project, Tokyo Dental College, Tokyo, Japan

3 Department of Pediatric Dentistry, Tokyo Dental College, Tokyo, Japan

4 Department of Anatomy, Tokyo Dental College, Tokyo, Japan

5 Department of Histology and Developmental Biology, Tokyo Dental College, Tokyo, Japan

Published online: 09 January 2025

other symptoms, and mutations in the *Alpl* gene were found in 57% of the patients [7]. The incidence of HPP is estimated to be approximately 1/100,000, and it is considered a rare disease with a low incidence [8]. However, recently, this low incidence has been attributed to the incidence of severe perinatal- and infantile-type HPP, with an actual incidence of approximately 1/6370 to 1/508. This suggests that mild-type HPP is not accurately diagnosed [8–10].

If a diagnosis of osteoporosis is made without a diagnosis of HPP, treatment may be harmful. It has been pointed out that if bisphosphonate preparations (BPs) are used incorrectly in patients with HPP, they may worsen osteomalacia or increase the risk of atypical fractures [11–14]. This is suggested to be due to a decrease in bone turnover [15]. Additionally, because the structure of BP is similar to that of pyrophosphate [16], a substrate for alkaline phosphatase and a mineralization inhibitor, the mineralization inhibitory effect may be exacerbated [13]. However, the corresponding details remain unclear.

Therefore, the purpose of this study was to administer zoledronic acid (Zol), a BP, to mice with mild-type HPP (Mouse *Alpl* gene = *Akp2*), analyze its effects on the femur, and measure the amount of spontaneous locomotor activity.

Methods

Animal Procedures

All experiments were approved by the Recombinant DNA Experiment Safety Committee and Animal Research Ethics Committee at Tokyo Dental College (DNA2101 and No. 300706). Mild-type HPP often exhibits autosomal dominant inheritance with a pathogenic mutation in only one allele, and heterozygous *Akp2*$^{+/-}$ mice are commonly used as a model for mild-type HPP [17]. Immediately after birth, genotyping was performed using forward, 5′-AGTCCGTGG GCATTGTGACTA-3′, and reverse, 5′-TGCTGCTCCACT CACGTCGAT-3′ primers according to the method previously reported, and *Akp2*$^{+/+}$ and *Akp2*$^{+/-}$ mice were distinguished [18]. First, we investigated the distribution of the BP preparations within the femurs of *Akp2*$^{+/-}$ mice. We used Zol-FAM (BioVinc LLC, CA, USA), a BP in which zoledronic acid (Zol) is labeled with the fluorescent substance FAM (FAM-Zol). FAM-Zol was diluted with physiological saline (PBS) and subcutaneously administered to 4-week-old *Akp2*$^{+/+}$ or *Akp2*$^{+/-}$ mice at 200 µg/kg (volume: 100 µL), and femurs were collected 24 h later [19].

Next, we investigated the effects of long-term administration of zoledronic acid hydrate on the femurs of *Akp2*$^{+/-}$ mice. Zol (Novartis, Basel, Switzerland) 1 mg/kg (volume: 200 µL) diluted in PBS was administered subcutaneously to 4-week-old *Akp2*$^{+/+}$ or *Akp2*$^{+/-}$ mice [20, 21]. The mice were administered the drug once a week until they were 8 weeks old (five times total), and sampling was performed at 9 weeks of age. *Akp2*$^{+/+}$ or *Akp2*$^{+/-}$ mice administered with the same amount of PBS were used as controls.

Distribution of BPs

The sampled femurs were cut into upper (containing the femoral head) and lower (containing the growth plate) sections. The samples were fixed using 4% paraformaldehyde (PFA) at 4 °C for 1 day. Sucrose substitution was performed, and the samples were encapsulated in Super Cryoembedding Medium (Leica Microsystems, Wetzlar, Germany) without decalcification. According to the Kawamoto method, the specimen was sliced to a thickness of 10 µm and attached to a Cryofilm Type IIC (9) (Leica Microsystems, Wetzlar, Germany). Hoechst 33342 solution (DOJINDO LABORATORIES, Kumamoto, Japan) was diluted 1/1000 for nuclear staining and mounted with SCMM-G1 (Leica Microsystems, Wetzlar, Germany), a glycerin-based mounting medium. The thin sections were mounted on MAS-coated glass slides (Matsunami Glass, Tokyo, Japan) and observed under a confocal microscope LSM880 (Carl Zeiss AG, Jena, Germany) ($n = 3$).

Histological Analysis

Harvested femurs were fixed in 0.1 M phosphorus acid buffer (pH 7.4) containing 4% paraformaldehyde (FUJIFILM Wako Pure Chemical Corporation, Osaka, Japan). They were decalcified in 10% ethylenediaminetetraacetic acid (Muto Junyaku, Tokyo, Japan) for 3 weeks, dehydrated in alcohol, cut into the upper part containing the femoral head and the lower part containing the growth plate, and embedded in paraffin. The prepared paraffin blocks were sectioned into serial sections of 4 µm thickness using a rotary microtome SM2000R (Leica Microsystems, Wetzlar, Germany). Thin sections were stained with hematoxylin–eosin (HE) staining (FUJIFILM Wako Pure Chemical Corporation, Osaka, Japan) to confirm tissue morphology. The sections were stained with Alcian blue (FUJIFILM Wako Pure Chemical Corporation, Osaka, Japan) to detect the chondrocyte matrix. Additionally, a TRAP/ALP Staining Kit (FUJIFILM Wako Pure Chemical Corporation, Osaka, Japan) was used to identify the osteoclasts. Photographs were captured using an Axio Imager M2 upright microscope (Carl Zeiss AG; $n = 3$).

Micro-computed Tomography Imaging

Harvested femurs were stored in 4% PFA at 4 °C overnight and fixed, and micro-computed tomography (micro-CT) imaging was performed. Two bone samples were excluded

from the study due to accidental breakage during sampling. The femoral head was imaged using a micro-CT50 (JEOL/SCANCO, Tokyo, Japan). Imaging conditions were as follows: tube voltage, 70 kV; tube current, 57 μA; voxel size, 14.8 × 14.8 × 14.8 μm. The growth plate area was imaged using a CosmoScan FX (Summit Pharmaceuticals International Corporation, Tokyo, Japan). Imaging conditions were as follows: tube voltage, 90 kV; tube current, 88 μA; voxel size, 10 × 10 × 10 μm. The captured data were imaged using software TRI/3D-SRF (Ratoc System Engineering, Tokyo, Japan; $n = 6$).

Bone Morphology Analysis

Based on the micro-CT images taken above, trabecular bone (TB) and cortical bone (CB) morphometry were performed using a 2-mm-thick area 0.5 mm away from the growth plate as the region of interest. Bone mineral density (BMD), bone mineral content (BMC), bone volume/tissue volume (BV/TV), trabecular thickness (Tb.Th), trabecular number (Tb.N), trabecular separation (Tb.Sp), trabecular spacing (Tb.Spac), marrow space star volume (V* m.space), average cortical thickness (Ct.Th), and cortical area fraction (Ct.Ar), which are used as typical bone morphometry parameters, were automatically calculated according to the TRI/3D-SRF software (Ratoc System Engineering) manual ($n = 6$).

Measurement of ALP Activity, P1NP, CTX-1, and α-SMA

Blood collected from the inferior vena cava at 9 weeks of age was left at room temperature for 30 min and then centrifuged at 4 °C and 12,000 rpm for 15 min to obtain the serum. The collected bone marrow of the femur was flushed with PBS, and the remainder was placed in a Cell-Cover solution (Anacyte Laboratories, Hamburg, Germany) and stored at 4 °C overnight. Thereafter, the cells were homogenized using EzRIPA Lysis Buffer (ATTO Corporation, Tokyo, Japan) to obtain a protein extract. The obtained serum and protein extract were used to measure ALP activity; procollagen 1 intact N-terminal propeptide (P1NP), a bone formation marker; type I collagen cross-linked C-terminal telopeptide (CTX-1), a bone resorption marker; and alpha-smooth muscle actin (α-SMA), a myofibroblast marker. As previously reported, ALP activity was determined by measuring the wavelength at 405 nm, taking advantage of its ability to convert the substrate *p*-nitrophenol phosphate to the strong yellow-soluble product *p*-nitrophenol under alkaline conditions. The amount of enzyme required to catalyze the production of 1 μmol p-nitrophenol per min was calculated as 1 U. Measurements were carried out using the MBS3805180 PINP ELISA Kit (MyBioSource Inc., San Diego, CA, USA) for P1NP, the AC-06FI CTX-1 ELISA kit (RatLapsTM, Immunodiagnostic System Ltd, Boldon, United Kingdom) for CTX-1, and the NBP2-66429 α-SMA ELISA kit (Novus Biologicals, Colorado, USA) for α-SMA according to the attached protocols. Protein concentrations of the serum and protein extracts were measured using a DC Protein Assay Kit (Bio-Rad, Hercules, CA, USA), and each measurement result was corrected to a value per milligram ($n = 5$).

RNA Extraction and Real-Time PCR

The collected femurs were pretreated in the same manner as for the protein extracts described prior. RNA was extracted using a RNeasy Mini Kit (QIAGEN, Hilden, Germany), according to the manufacturer's instructions. The extracted RNA was immediately synthesized into cDNA using SuperScript® Reverse Transcriptase (Thermo Fisher Scientific, Massachusetts, USA) with random hexamers. Relative quantification by the ΔΔCT method was then performed using QuantStudio 7Pro (Applied Biosystems, Massachusetts, USA). *Runx2*, *sp7*, *col1a1*, *Bglap*, and *col2a1* were measured on TB Green® Premix Ex Taq™ II (Clontech Laboratories, TaKaRa Bio Company, Ohtsu, Shiga, Japan) using the primers shown in Supplementary Table 1, and the remaining *Alpl*, *BMP2*, cartilage oligomeric matrix protein (*COMP*), *col10a1*, CCAAT/Enhancer Binding Protein-β (*C/*EBPβ), and Smad ubiquitination regulatory factors-2 (*Smurf2*) were measured using a custom TaqMan® array plate from Thermo Fisher Scientific. Both systems used *18S rRNA* as the endogenous control. Gene names and Assay IDs are listed in Supplementary Table 1. The obtained data were analyzed using ExpressionSuite ™ Software v1.3 (Applied Biosystems; $n = 5$).

Spontaneous Locomotor Activity

After the last Zol administration, 8-week-old mice underwent spontaneous locomotor activity measurements using a wheel cage RWC-15 (MELQUEST, Toyama, Japan). The amount of movement of the mice was measured for the activity time, total distance, average speed, and acceleration for 3 days, and the average values were calculated from the results on the second and third days, excluding the first day as a training period. The average speed was calculated by averaging the values, excluding those where the distance traveled per minute was zero, and the maximum value was calculated for acceleration. The average speed was detected using the momentum data recording and analysis system CIF-4S (MELQUEST) and analyzed using the Actmaster software (MELQUEST) ($n = 8$).

Statistical Analysis

All data are presented as the mean ± SD. Statistical analyses were performed using the Prism 10 software (GraphPad Software, La Jolla, CA, USA). Significant differences between two groups were analyzed using an unpaired two-tailed Student's *t* test. Significant differences among the four groups were determined using two-way ANOVA and Šídák's multiple comparison tests. Statistical differences were considered significant at $P < 0.05$, and statistical analyses and graphing were performed using Prism 10 (GraphPad Software, La Jolla, CA, USA).

Results

No Difference was Observed in the Distribution of Zol Between *Akp2*$^{+/+}$ and *Akp2*$^{+/-}$ Mice

Akp2$^{+/-}$ mice have a mutation in the *Alpl* gene in one allele; therefore, they are a common mouse model for mild-type HPP syndrome, which is often inherited in an autosomal dominant manner [17, 22]. Similar to the clinical phenotype of mild HPP, *Akp2*$^{+/-}$ mice showed delayed calcification and hypoplasia (Supplementary Fig. S1a–c).

FAM-Zol was subcutaneously administered to *Akp2*$^{+/+}$ and *Akp2*$^{+/-}$ mice, and the following day, the femurs were sampled, sections were prepared, and the distribution of Zol was examined by confocal microscopy. There was no difference between *Akp2*$^{+/+}$ and *Akp2*$^{+/-}$ mice, and Zol was distributed to the femur on the day after administration. There was no difference between the two groups in distribution within the femur, and Zol was distributed on the cortical bone surface, cancellous bone surface, and perichondrium. In particular, it was strongly distributed directly beneath the growth plate and subchondral bone (Fig. 1a–d).

Femoral Head Cartilage Rupture Upon Zol Treatment in *Akp2*$^{+/-}$ Mice

Damage and tearing of the femoral head cartilage was observed in *Akp2*$^{+/-}$ mice, in which Zol was administered subcutaneously (Fig. 2d). No abnormal findings, such as

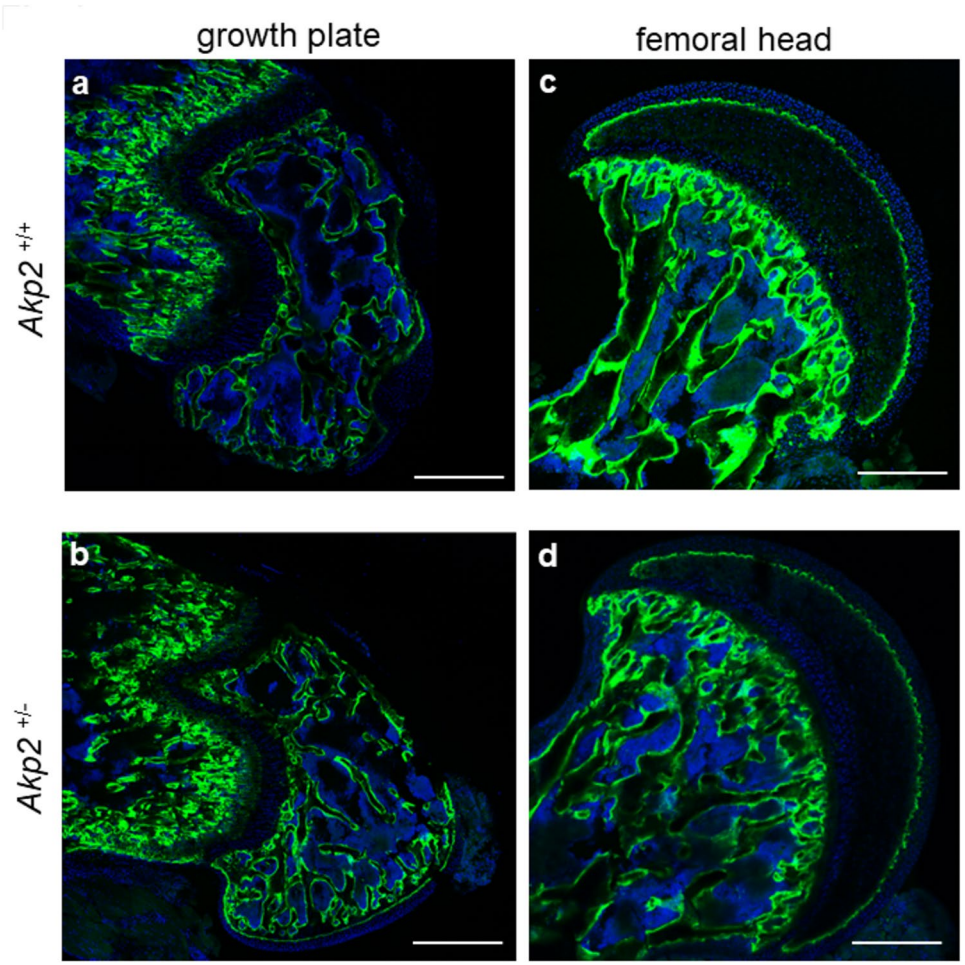

Fig. 1 Distribution of Zol in the femur. Zoledronic acid hydrate (Zol) conjugated with the fluorescent dye FAM (FAM-Zol) was subcutaneously administered to 4-week-old *Akp2*$^{+/+}$ or *Akp2*$^{+/-}$ mice, and its distribution was confirmed. The green part shows the area where FAM-ZOL was distributed, and the blue part shows the nuclear staining area. **a** Growth plate of *Akp2*$^{+/+}$ mice. Scale bars, 1 mm. **b** Growth plate of *Akp2*$^{+/-}$ mice. Scale bars, 1 mm. **c** Femur head of *Akp2*$^{+/+}$ mice. Scale bars, 400 µm. **d** Femur head of *Akp2*$^{+/-}$ mice. Scale bars, 400 µm

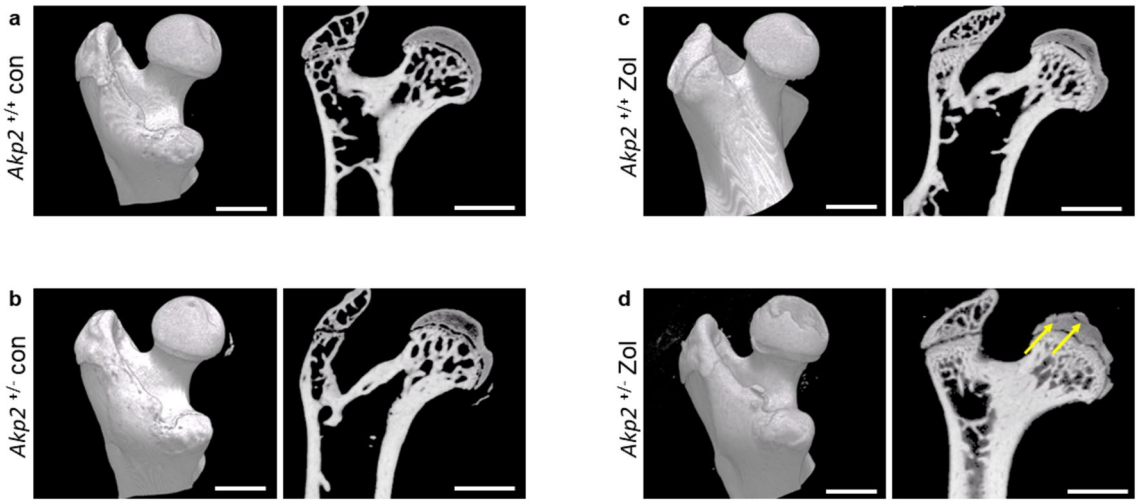

Fig. 2 3D and tomographic images of the femoral head. Zoledronic acid hydrate (Zol) was subcutaneously administered once a week from week 4 to week 8 for a total of 5 times, and the femoral head was photographed using micro-CT to construct 3D (diagram on the left) and tomographic images (diagram on the right). **a** Control $Akp2^{+/+}$ mice. Scale bars, 1 mm. **b** Control $Akp2^{+/-}$ mice. Scale bars, 1 mm. **c** Zol-treated $Akp2^{+/+}$ mice. Scale bars, 1 mm. **d** Zol-treated $Akp2^{+/-}$ mice. The yellow arrow indicates the area where rupture of the femoral head cartilage was confirmed. Scale bars, 1 mm

tears, were observed in the other groups, and their corresponding morphologies were normal (Fig. 2a–c).

For a more detailed analysis, paraffin sections were prepared and subjected to three types of staining: hematoxylin and eosin (HE), Alcian blue, and TRAP/ALP staining, and histological observation was performed. There was no particular difference between control $Akp2^{+/+}$ and $Akp2^{+/-}$ mice, and many multinucleated TRAP-positive cells were observed in the growth cartilage zone of the femoral head (Fig. 3a, b). In the groups in which Zol was subcutaneously administered to $Akp2^{+/+}$ and $Akp2^{+/-}$ mice, the femoral head cartilage was more strongly stained with Alcian blue than in the control group. In addition, TRAP/ALP staining revealed a decrease in TRAP-positive cells, and most of the stained cells were mononuclear (Fig. 3c, d). Furthermore, in the group in which Zol was subcutaneously administered to $Akp2^{+/-}$ mice, the fibrous tissue that was not stained with Alcian blue but deeply stained with eosin was observed at the ruptured site of the femoral head cartilage. Nuclei were observed in this fibrous tissue (Fig. 3d).

Zol Administration Promotes Bone Formation in *Akp2*$^{+/-}$ but to a Lesser Effect Than in *Akp2*$^{+/+}$ Mice

Micro-CT imaging near the femoral growth plate showed that control $Akp2^{+/-}$ mice had less trabecular bone and numerous low-density green areas in the cortical bone BMD images than control $Akp2^{+/+}$ mice (Fig. 4a, b). When Zol was administered, the bone marrow was filled with trabecular bone compared to the control group. However, even in the same Zol administration group, the amount was smaller in $Akp2^{+/-}$ mice than in $Akp2^{+/+}$ mice, and more low-density light blue was observed in the BMD images (Fig. 4c, d). BMD and BMC measurements were considerably higher when Zol was administered compared to those in the control groups.

BMD and BMC measurements were significantly higher in Zol-treated mice than those in control mice, except for the comparison of TB BMD between control and Zol-treated $Akp2^{+/-}$ mice. Additionally, TB BMD, CB BMD, and CB BMC measurements were significantly lower in Zol-treated $Akp2^{+/-}$ mice compared to those in Zol-treated $Akp2^{+/+}$ mice (Fig. 4e–h). However, for TB BMC, Zol-treated $Akp2^{+/-}$ mice tended to have higher values than Zol-treated $Akp2^{+/+}$ mice, although the difference was not significant (Fig. 4g). Similarly, the results of BV/TV and Tb.Th indicated significantly higher values in the Zol-treated group than in the control group, with the Zol-treated $Akp2^{+/-}$ mice exhibiting significantly lower values than those of the Zol-treated $Akp2^{+/+}$ mice (Fig. 4i, j). For Tb.N, control $Akp2^{+/-}$ mice exhibited significantly lower values than those in control $Akp2^{+/+}$ mice; however, there was no significant difference between Zol-treated $Akp2^{+/-}$ and Zol-treated $Akp2^{+/+}$ mice (Fig. 4k). Moreover, Tb.Sp, Tb.Spac, and V* m.space were significantly lower in the Zol-treated groups than in the control groups. Tb.Sp was extensively higher in Zol-treated $Akp2^{+/-}$ mice than in Zol-treated $Akp2^{+/+}$ mice (Fig. 4l). Although, Tb.Spac and V* m.space values were significantly higher in control $Akp2^{+/-}$ mice than in control $Akp2^{+/+}$ mice, there was no significant difference between Zol-treated $Akp2^{+/-}$ mice and Zol-treated $Akp2^{+/+}$ mice (Fig. 4m, n). In the cortical bone analysis, no difference was observed in Ct.Th between all groups; however, Ct.Ar was markedly

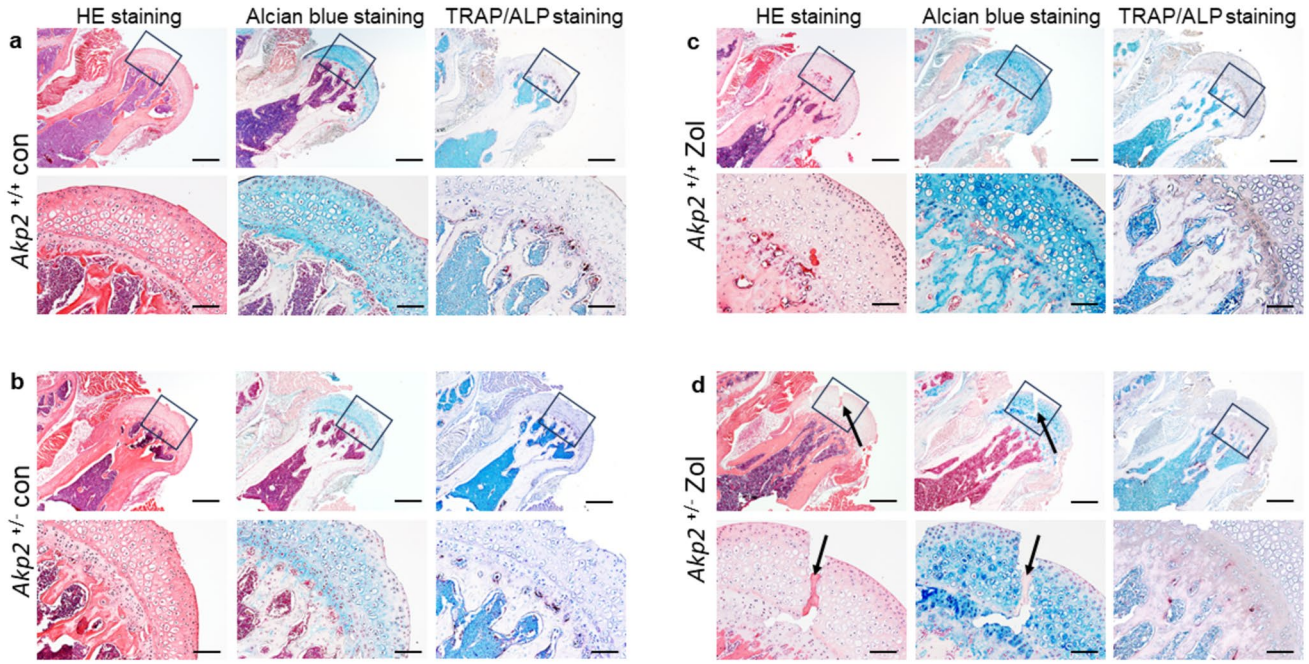

Fig. 3 Histological findings of the femoral head. Histological findings of the femoral head treated with zoledronic acid hydrate (Zol) for 5 weeks. The image on the left shows hematoxylin and eosin staining, that in the middle shows Alcian blue staining, and that on the right shows TRAP/ALP staining. The top image shows the overall image of the femoral head (Scale bars, 400 μm), and the bottom image shows a high view (Scale bars, 100 μm) of the area surrounded by the black square in the top image. **a** Control *Akp2*$^{+/+}$ mice. **b** Control *Akp2*$^{+/-}$ mice. **c** Zol-treated *Akp2*$^{+/+}$ mice. **d** Zol-treated *Akp2*$^{+/-}$ mice. The area indicated by the black arrow indicates the area where fibrous tissue was confirmed

higher in the Zol-treated groups than in the control groups, similar to the trabecular bone analysis. However, this value was significantly lower in Zol-treated *Akp2*$^{+/-}$ mice than in Zol-treated *Akp2*$^{+/+}$ mice (Fig. 4o, p).

Differences in Bone-Like Structure Below the Growth Plate Following Zol Administration

No particular histological differences were observed between control *Akp2*$^{+/+}$ and *Akp2*$^{+/-}$ mice, and in both groups, many multinucleated TRAP-positive cells were confirmed just below the growth plate and on the trabecular bone surface (Fig. 5a, b). When Zol was administered, bone-like structures were formed just below the growth plate in both *Akp2*$^{+/+}$ and *Akp2*$^{+/-}$ mice, but unlike normal cancellous bone, they contained many nuclei. Furthermore, the inner matrix was deeply stained with Alcian blue. In addition, many mononuclear TRAP-positive cells were observed in the bone-like structure (Fig. 5c, d).

Administration of Zol Decreased Bone Formation and Bone Resorption Markers

Regarding ALP activity, which is an indicator marker of HPP, control *Akp2*$^{+/-}$ mice had considerably lower values than control *Akp2*$^{+/+}$ mice. In addition, ALP activity in the protein extracts markedly decreased when Zol was administered (Fig. 6a, e). Compared to control *Akp2*$^{+/+}$ mice, Zol-treated *Akp2*$^{+/-}$ mice had considerably lower levels of P1NP and CTX-1. In particular, the value of CTX-1 in the protein extract was even lower in Zol-treated *Akp2*$^{+/-}$ mice compared to that in Zol-treated *Akp2*$^{+/+}$ mice (Fig. 6b, c, f, g). Furthermore, α-SMA showed different trends in serum and protein extracts. Serum α-SMA was considerably higher in Zol-treated *Akp2*$^{+/-}$ mice than in control *Akp2*$^{+/-}$ mice (Fig. 6d). However, α-SMA in the protein extract, like other bone markers, was markedly lowered upon the administration of Zol (Fig. 6h).

Administration of Zol to Akp2$^{+/-}$ Mice Increases C/EBPβ and Smurf2

To investigate this underlying mechanism, bone formation-related marker genes (*Runx2*, *Alpl*, *sp7*, *col1a1*, *Bglap*, and *BMP2*) and cartilage marker genes (*col2a1* and *COMP*) were investigated. *C/EBPβ*, which is involved in cartilage degeneration, and *Smurf2*, which controls bone induction, were measured using real-time PCR. In terms of *Runx2*, *Alpl*, and *sp7*, bone formation markers, Zol-treated *Akp2*$^{+/-}$ mice exhibited considerably higher expression levels than those

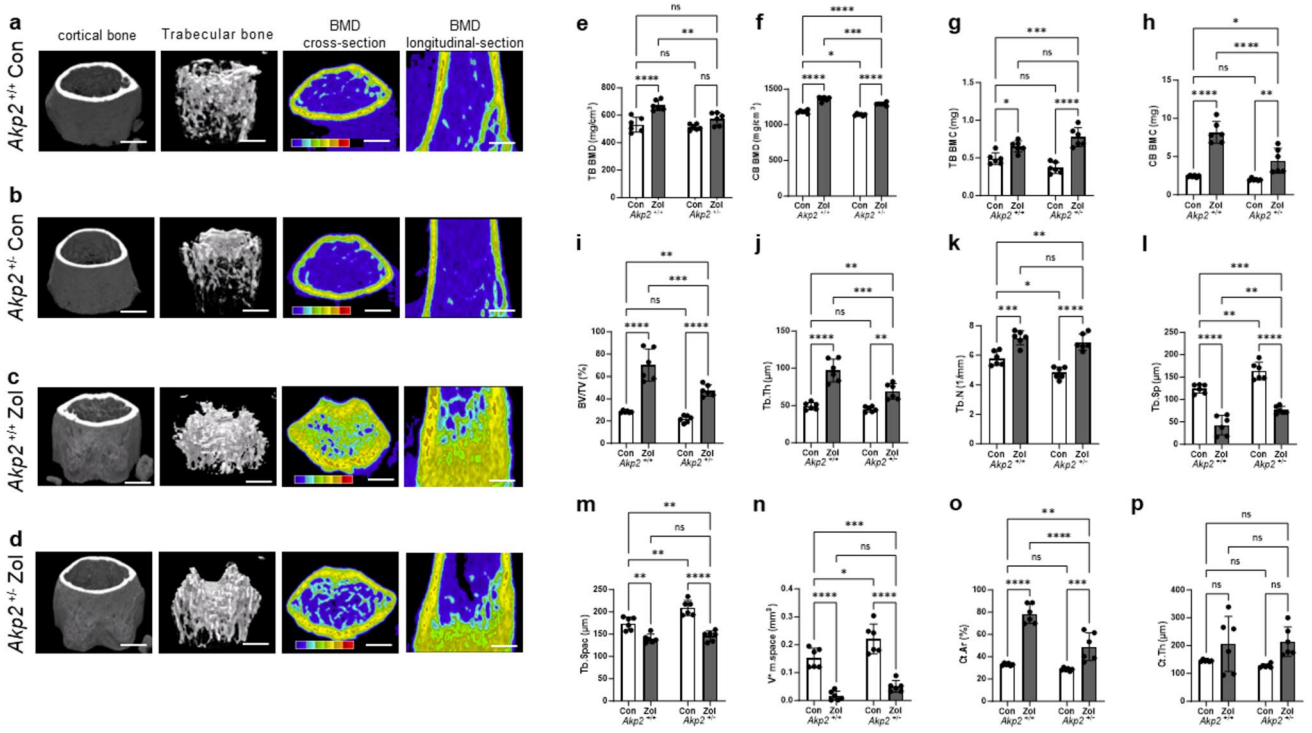

Fig. 4 Micro-CT image and bone morphology analysis of a femoral growth plate upon Zol administration. Images were taken 2 mm above each femoral growth plate, excluding 0.5 mm, using micro-CT, and images were constructed using the TRI/3D-SRF software (**a**–**d**). The left panel shows cortical bone extraction images, trabecular bone extraction images, BMD cross-sectional images, and BMD longitudinal sectional images. Scale bars are 0.5 mm, and the color scale is blue for low-density BMD values, yellow for medium density, and red for high density. Regarding the same region of interest, bone morphometry was also performed using TRI/3D-SRF (**e**–**p**). Dots indicate the respective values; error bars represent SD ($n=6$). *$P<0.05$, **$P<0.01$, ***$P<0.005$, ****$P<0.001$. *ns* not significant

of control *Akp2*$^{+/-}$ mice. In particular, *Runx2* and *BMP2* expression levels were markedly higher in Zol-treated *Akp2*$^{+/-}$ mice than in Zol-treated *Akp2*$^{+/+}$ mice (Fig. 7a–f). The expression of *Col2a1*, a cartilage collagen marker, was markedly decreased upon the administration of Zol compared to that in the control (Fig. 7g). Conversely, regarding the cartilage non-collagen glycoproteins *COMP*, *C/EBPβ*, and *Smurf2*, Zol-treated *Akp2*$^{+/-}$ mice had considerably higher values than those of the other groups (Fig. 7h–j).

Administration of Zol to *Akp2*$^{+/-}$ Mice Reduced Spontaneous Locomotor Quality

The mice in all groups were visually indistinguishable and in good health, with no significant differences in body weight (Supplementary Fig. S2).

Spontaneous locomotor activity showed no difference in activity time between the groups (Fig. 8a). Nevertheless, the total distance, average velocity, and acceleration were considerably lower in Zol-treated *Akp2*$^{+/-}$ mice than in control *Akp2*$^{+/+}$ mice. In particular, regarding the total distance traveled and average speed, Zol-treated *Akp2*$^{+/-}$ mice had lower values than Zol-treated *Akp2*$^{+/+}$ mice (Fig. 8b–d).

Discussion

As a result of subcutaneous administration of Zol to *Akp2*$^{+/-}$ mice, rupture was observed in the femoral head cartilage, and bone formation directly below the femoral growth plate was found to be less than that in normal-type mice. Furthermore, it was found that *C/EBPβ*, a marker of cartilage degeneration, and *Smurf2*, which suppresses BMP osteoinduction, were considerably elevated in the femurs of Zol-treated *Akp2*$^{+/-}$ mice. A decline in the quality of spontaneous locomotor activity was also observed.

First, regarding the femoral head, when Zol was administered to the *Akp2*$^{+/-}$ mice, a tear was observed in the femoral head cartilage, and a fibrous structure was found to have wandered into the tear site. Because nuclei were present in this fibrous structure, we suspected fibrosis caused by myofibroblasts. Therefore, when we quantified the amount of α-SMA, a myofibroblast marker, in the serum, it was found to be high in Zol-treated *Akp2*$^{+/-}$ mice. Furthermore, *col2a1*, a fibrous component of normal cartilage, was considerably lowered upon Zol administration. *COMP*, a cartilage non-collagen glycoprotein, was markedly higher in Zol-treated *Akp2*$^{+/-}$ mice than in Zol-treated *Akp2*$^{+/+}$ mice,

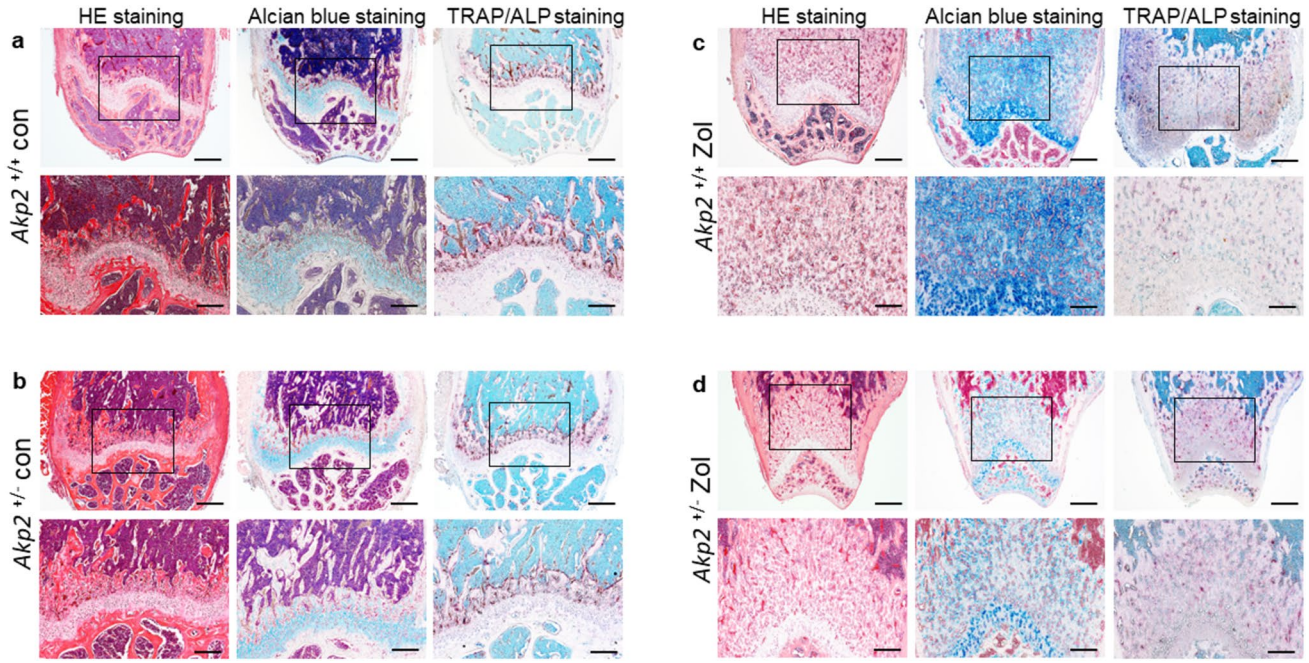

Fig. 5 Histological findings of a femoral growth plate upon Zol administration. The image on the left shows hematoxylin and eosin staining, that in the middle shows Alcian blue staining, and that on the right shows TRAP/ALP staining. The top image shows the overall image of the femoral head (Scale bars, 400 μm), and the bottom image shows a high view (Scale bars, 200 μm) of the area surrounded by the black square in the top image. **a** Control *Akp2*$^{+/+}$ mice. **b** Control *Akp2*$^{+/-}$ mice. **c** Zol-treated *Akp2*$^{+/+}$ mice. **d** Zol-treated *Akp2*$^{+/-}$ mice

and *C/EBPβ*, a maker of cartilage degeneration [23, 24], was also higher in *Akp2*$^{+/-}$ mice treated with Zol. Based on these results, we hypothesized that the BMD of the acetabulum, which comprises the socket for the femoral head and the subchondral bone part of the femoral head, increased after Zol administration, resulting in excessive mechanical stress. It has been reported that COMP expression increases in areas subjected to excessive mechanical stress, such as cartilage tissue damage sites due to osteoarthritis, to protect the cartilage [25, 26]. The increase in COMP that occurs only in Zol-treated *Akp2*$^{+/-}$ mice confirms that excessive mechanical stress is applied. The cartilage of *Akp2*$^{+/-}$ mice was unable to cope with this excessive mechanical stress and degenerated; furthermore, continued mechanical stress resulted in rupture of the femoral head cartilage, necessitating repair by muscle fibers.

Next, regarding changes in the bone near the growth plate, the bone marrow area directly below the growth plate was filled with bone-like structures in both *Akp2*$^{+/+}$ and *Akp2*$^{+/-}$ mice due to the administration of Zol. Considering the density of the micro-CT image, the bone-like structure that formed just below the femoral growth plate appeared similar to bone. However, it contained numerous nuclei and stained deeply with Alcian blue. These characteristics reveal that the properties of this bone-like structure are clearly different from those of the normal trabecular bone. Chondroid bone is a calcified tissue in which chondroid-like cells are surrounded by a bone matrix and has been reported to possess properties of both cartilage and bone [27]. It is formed in areas where mechanical stress is applied and bone formation progresses rapidly [28]. Thus, we interpreted that the chondroid bone formed just below the growth plate and that bone resorption was inhibited upon BP administration, resulting in rapid bone formation.

In addition, the results of morphometric measurements using micro-CT revealed that seven parameters—CB BMD, TB BMC, CB BMC, BV/TV, Tb.Th, Tb.N, and Ct.Ar—were significantly higher in Zol-treated *Akp2*$^{+/-}$ mice than in control *Akp2*$^{+/-}$ mice. Although TB BMD also tended to be higher in the Zol-treated group, the difference was no significant. Tb.Sp, Tb.Spac, and V* m.space were significantly lower in Zol-treated *Akp2*$^{+/-}$ mice than in control *Akp2*$^{+/-}$ mice. Although Tb.N, Tb.Spac, and V* m.space values were significant differences observed between control *Akp2*$^{+/-}$ mice and control *Akp2*$^{+/+}$ mice, there were no differences between Zol-treated *Akp2*$^{+/-}$ mice and Zol-treated *Akp2*$^{+/+}$ mice. At the RNA level, the expression of *Runx2*, *Alpl*, and *sp7*, bone formation markers, was considerably higher in Zol-treated *Akp2*$^{+/-}$ mice than in control *Akp2*$^{+/-}$ mice. In particular, *Runx2* and *BMP2* expression levels were markedly higher in Zol-treated *Akp2*$^{+/-}$ mice than in Zol-treated *Akp2*$^{+/+}$ mice. These results were

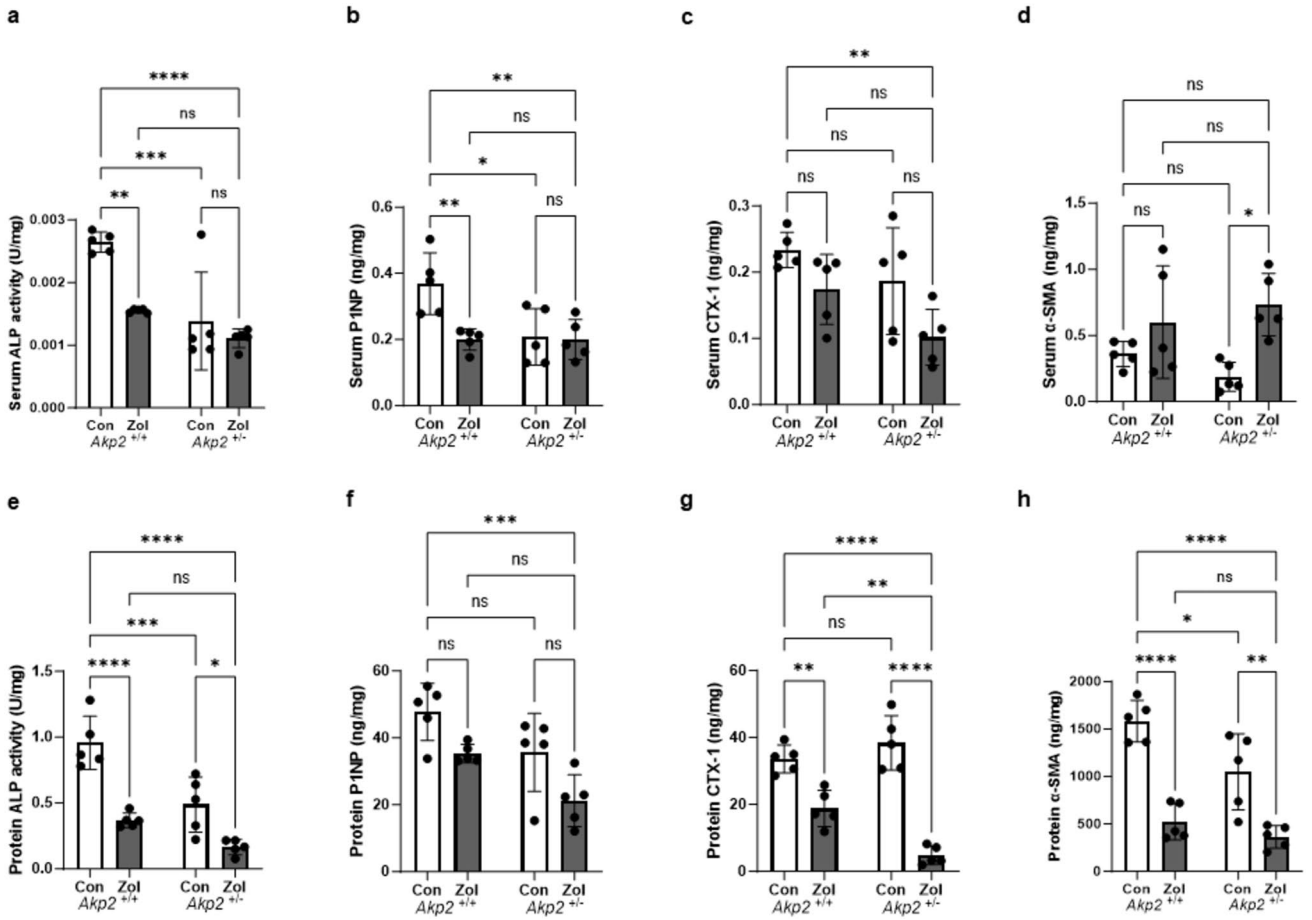

Fig. 6 Changes in various markers upon Zol administration. We quantified the changes in various markers in the serum and protein extracts from the femur when Zol was administered. Serum and protein extracts were measured for ALP with low HPP values; P1NP, a bone formation marker; CTX-1, a bone resorption marker; and α-SMA, a myofibroblast proliferation marker. Dots indicate the respective values; error bars represent SD ($n=5$). $*P<0.05$, $**P<0.01$, $***P<0.005$, $****P<0.001$. *ns* not significant

presumed to be due to the therapeutic effects of Zol. On the other hand, six parameters—TB BMD, CB BMD, CB BMC, BV/TV, Tb.Th, and Ct.Ar—were significantly lower in Zol-treated *Akp2*$^{+/-}$ mice than in Zol-treated *Akp2*$^{+/+}$ mice. Furthermore, Tb.Sp was higher in Zol-treated *Akp2*$^{+/-}$ mice than in Zol-treated *Akp2*$^{+/+}$ mice. If the previously suggested mechanism is correct—that the calcification inhibitory effect is promoted due to the structural similarity between pyrophosphate, a calcification inhibitor, and bisphosphonates (BPs)—then the bone morphometry results of the Zol-treated *Akp2*$^{+/-}$ mice would be lower than those of the control *Akp2*$^{+/-}$ mice. Additionally, some bone morphometry results showed lower values in Zol-treated *Akp2*$^{+/-}$ than in Zol-treated *Akp2*$^{+/+}$ mice. Therefore, we hypothesized that compared to control *Akp2*$^{+/-}$ mice, bone formation in Zol-treated *Akp2*$^{+/-}$ mice progresses toward enhancement but decreases compared to that in *Akp2*$^{+/+}$ mice, which may have occurred as a result of a mechanism that is not yet clear. We analyzed the gene expression level of *Smurf2*, which has been shown to suppress the BMP/Smad signal [29, 30], and found that it was considerably higher only in Zol-treated *Akp2*$^{+/-}$ mice. Thus, bone formation due to the administration of Zol was promoted in both *Akp2*$^{+/+}$ and *Akp2*$^{+/-}$ mice, but bone formation was partially suppressed in *Akp2*$^{+/-}$ mice treated with Zol due to *Smurf2*. Therefore, we believe that bone formation is reduced in Zol-treated *Akp2*$^{+/-}$ mice compared to that in Zol-treated *Akp2*$^{+/+}$ mice.

Finally, we conducted spontaneous locomotor activity analysis to determine whether these changes were simply histological or had a negative impact on athletic performance. As a result, Zol-treated *Akp2*$^{+/-}$ mice had lower total distance and average speed compared to Zol-treated *Akp2*$^{+/+}$ mice, despite having the same activity time. Therefore, the changes in Zol-treated *Akp2*$^{+/-}$ mice described above appeared to result in a decline in the quality of spontaneous locomotor activity.

Based on these results, the statement that BP administration should be avoided for patients with HPP, which is

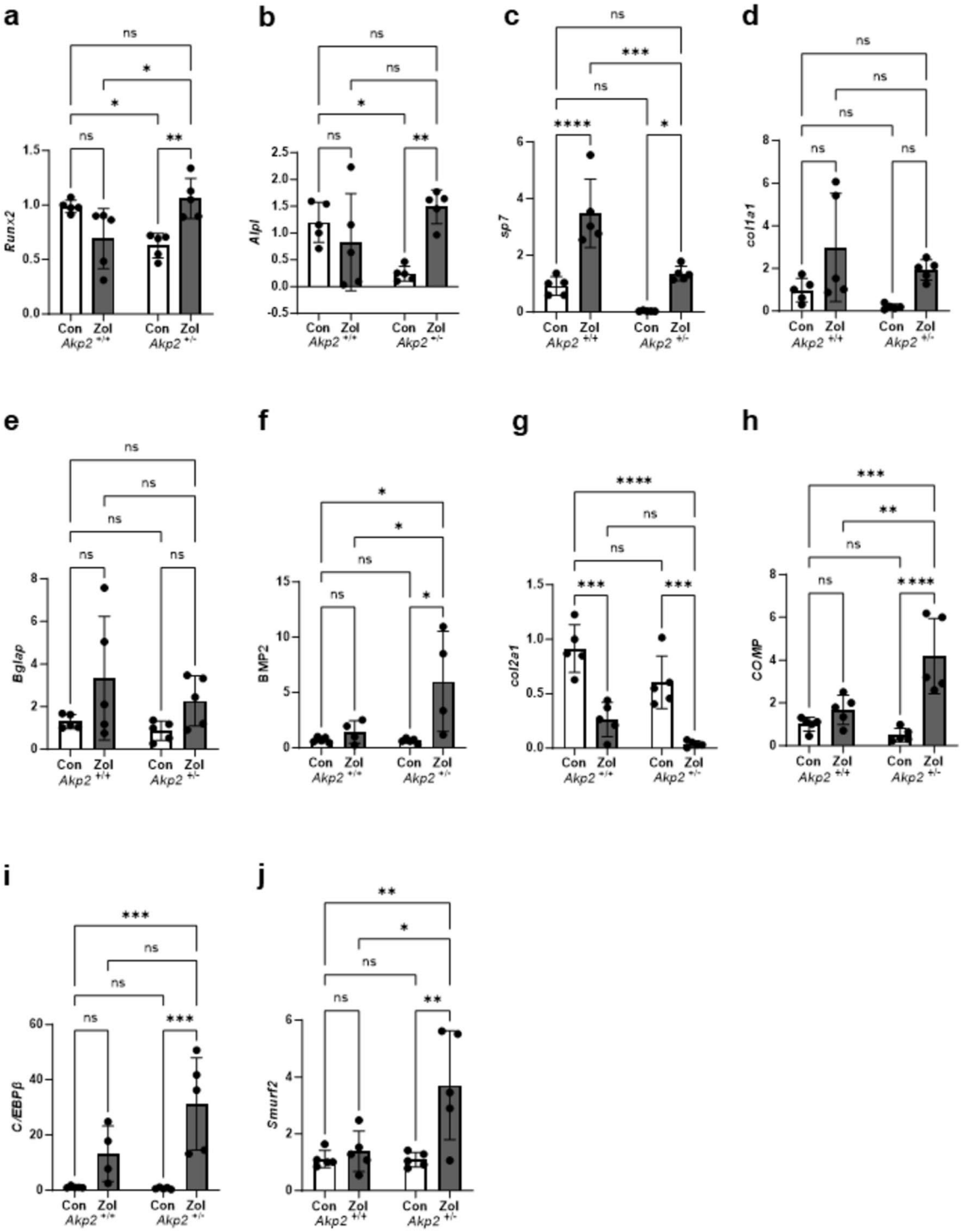

Fig. 7 Changes in various markers of cDNA. RNA was extracted from the femurs treated with Zoledronic acid hydrate and converted to cDNA, and relative quantification of bone formation markers (*Runx2*, *Alpl*, *sp7*, *col1a1*, *bglap*, and *BMP2*) was performed using the ΔΔCT method. Similarly, each group was compared for col2a1 and COMP, which are cartilage components; C/EBP, which is said to be involved in articular cartilage degeneration; and Smurf2, which is said to suppress osteoinductive ability. Dots indicate the respective values; error bars represent SD ($n=5$). *$P<0.05$, **$P<0.01$, ***$P<0.005$, ****$P<0.001$. *ns* not significant

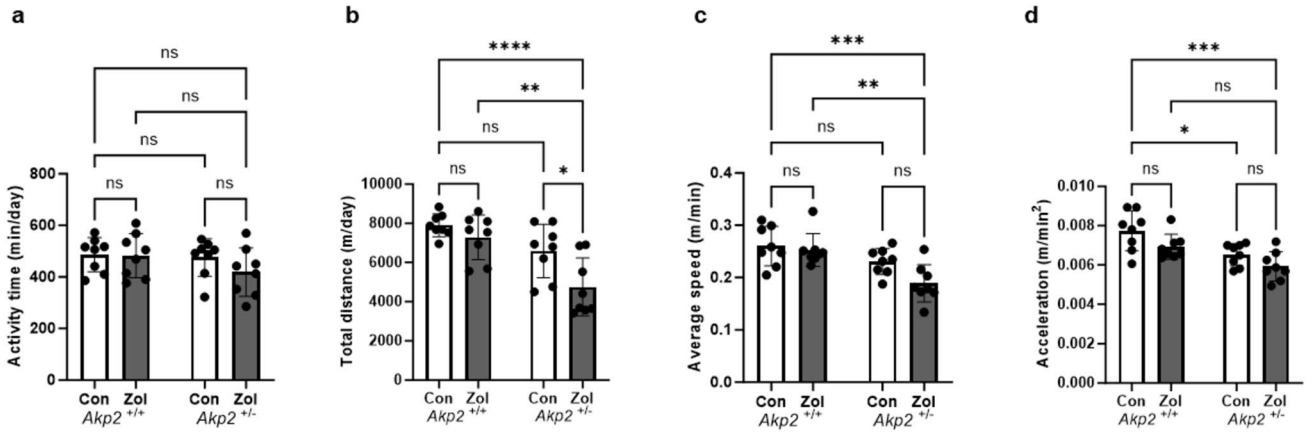

Fig. 8 Spontaneous movement analysis. After the administration of Zoledronic acid hydrate (8 weeks of age), the locomotor ability of the mice in each group was quantified using a wheel cage. **a** Activity time (min/day). **b** Total distance (m/day). **c** Average speed (m/min). **d** Acceleration (m/min^2). Dots indicate the respective values; error bars represent SD ($n=8$). *$P<0.05$, **$P<0.01$, ***$P<0.005$, ****$P<0.001$. *ns* not significant

included in the "Clinical Practice Guidelines for HPP" of the Japanese Pediatric Endocrine Society, is valid [31]. While HPP is highly recognized among obstetricians, gynecologists, pediatricians, and pediatric dentists, its recognition among doctors and dentists in other medical departments is extremely low [32]. When diagnosed with general osteoporosis, Japan's "2015 Guidelines for Prevention and Treatment of Osteoporosis" lists proximal femur fractures as fractures that should be prevented from the perspective of maintaining life prognosis and quality of life. Therefore, BPs are considered first-line drugs for patients at high risk of hip fracture [33]. To avoid administering BP to patients with HPP, it is important to accurately diagnose patients with mild HPP who do not exhibit typical symptoms. We believe that it is essential for people to be aware of the existence of HPP.

This study has some limitations. First, this experiment assumed that because patients with mild-type HPP repeatedly suffer from fractures at a relatively young age, BP administration would be started early, leading to greater accumulation in the bones. Therefore, the dose was rather high. In future research, it is necessary to investigate whether changing the dose would have the same effect. Second, although *Smurf2* has been suggested to be involved in bone changes near the growth plate in Zol-treated *Akp2*$^{+/-}$ mice, it remains unclear why *Smurf2* was increased only in Zol-treated *Akp2*$^{+/-}$ mice. Previous reports have suggested that ALP may act as an anti-inflammatory nucleotidase [34]. The lower ALP activity in *Akp2*$^{+/-}$ mice than in *Akp2*$^{+/+}$ mice might be due to a weaker anti-inflammatory effect; however, further verification is needed. Third, although there was no significant difference in TB BMC, Zol-treated *Akp2*$^{+/-}$ mice tended to have higher than Zol-treated *Akp2*$^{+/+}$ mice. This result is inconsistent with the imaging findings. This discrepancy arises because Zol-treated *Akp2*$^{+/+}$ mice have more areas where the cortical and TBs are continuous, which may lead to some of the trabecular bone being misidentified as CB. To address this issue, a more detailed analysis using micro-CT equipment that can distinguish between cancellous and cortical bones may be required.

Conclusion

When BP was administered to mice with mild-type HPP, rupture occurred in the femoral head cartilage. This was presumed to have occurred because excessive mechanical stress was generated by BP-induced bone hardening, resulting in cartilage degeneration. Furthermore, bone formation directly below the femoral growth plate was reduced compared with that in normal mice. This difference may be related to the inhibition of bone formation by *Smurf2*. In addition to these histological changes, a decline in the quality of spontaneous locomotor activity was also observed.

Supplementary Information The online version contains supplementary material available at https://doi.org/10.1007/s00223-024-01326-w.

Acknowledgements We thank Dr. Jose Luis Millán and Dr. Sonoko Narisawa at the Sanford-Burnham Medical Research Institute for providing the *Akp2*$^{-/-}$ mice. We would like to thank Editage (www.editage.jp) for English language editing.

Authors Contributions Aki Nakamura-Takahashi contributed toward conceptualization, methodology, validation, formal analysis, data curation, writing—original, visualization, supervision, project administration, and funding acquisition. Satoshi Ishizuka contributed toward formal analysis, visualization, conceptualization, writing—review & editing and funding acquisition. Kengo Hirai contributed toward formal analysis, conceptualization, and writing—review & editing. Satoru Matsunaga contributed toward conceptualization and writing—review

& editing. Norio Kasahara contributed toward conceptualization and writing—review & editing. Seikou Shintani contributed toward conceptualization and writing—review & editing. Shinichi Abe contributed toward conceptualization and writing—review & editing. Masataka Kasahara contributed toward conceptualization and writing—review & editing.

Funding Grants or Research Foundation: Aki Nakamura-Takahashi—this work was supported by JSPS KAKENHI [Grant Numbers JP19K18970 and 23K15986], Tokyo Dental College Research Branding Project, Tokyo Dental College Well-being Project, and Nakatomi Research Foundation. Satoshi Ishizuka—this work was supported by JSPS KAKENHI Grant Number JP22K17026. Payment or honoraria for lectures and Support for attending meetings and travel: Aki Nakamura-Takahashi—Part of this research was presented at 26th Annual meeting of Japanese Society of Hospital General Medicine Sponsored symposium (2/19/2023), 56th Annual musculoskeletal Tumor meeting of the Japanese Orthopaedic Association Sponsored symposium (7/13/2023), and 66th Autumn meeting of the Japanese Society of Periodontology Luncheon Seminar (10/13/2023) at the request of Alexion Pharma, and I received travel expenses, transportation costs, and honoraria from Alexion Pharma.

Conflict of Interest All authors have no conflicts of interest with respect to this study other than those stated in the Funding section.

Human and Animal Rights and Informed Consent This study was approved by the Tokyo Dental College Animal Experimentation Committee and the Recombinant DNA Experiment Safety Committee (approval numbers: 300706, DNA2101). The study protocol also complied with the ARRIVE guidelines.

References

1. Whyte MP (2016) Hypophosphatasia—aetiology, nosology, pathogenesis, diagnosis and treatment. Nat Rev Endocrinol 12(4):233–246
2. Whyte MP (2017) Hypophosphatasia: an overview for 2017. Bone 102:15–25
3. Khan AA et al (2019) Hypophosphatasia: Canadian update on diagnosis and management. Osteoporos Int 30(9):1713–1722
4. İnci A et al (2021) Hypophosphatasia: is it an underdiagnosed disease even by expert physicians? J Bone Miner Metab 39(4):598–605
5. Ng E et al (2023) A low serum alkaline phosphatase may signal hypophosphatasia in osteoporosis clinic patients. Osteoporos Int 34(2):327–337
6. Seefried L et al (2020) Burden of illness in adults with hypophosphatasia: data from the global hypophosphatasia patient registry. J Bone Miner Res 35(11):2171–2178
7. Feurstein J et al (2022) Identifying adult hypophosphatasia in the rheumatology unit. Orphanet J Rare Dis 17(1):435
8. Mornet E et al (2011) A molecular-based estimation of the prevalence of hypophosphatasia in the European population. Ann Hum Genet 75(3):439–445
9. Tournis S et al (2021) Hypophosphatasia. J Clin Med 10(23):5676
10. González-Cejudo T et al (2024) Mild hypophosphatasia may be twice as prevalent as previously estimated: an effective clinical algorithm to detect undiagnosed cases. Clin Chem Lab Med 62(1):128–137
11. Zhou W et al (2023) Prevalence of monogenic bone disorders in a Dutch cohort of atypical femur fracture patients. J Bone Miner Res 38(6):896–906
12. Whyte MP (2009) Atypical femoral fractures, bisphosphonates, and adult hypophosphatasia. J Bone Miner Res 24(6):1132–1134
13. Sutton RA et al (2012) "Atypical femoral fractures" during bisphosphonate exposure in adult hypophosphatasia. J Bone Miner Res 27(5):987–994
14. Cundy T et al (2015) Reversible deterioration in hypophosphatasia caused by renal failure with bisphosphonate treatment. J Bone Miner Res 30(9):1726–1737
15. McClung MR, Ebetino FH (2020) History of risedronate. Bone 137:115407
16. Kaboudin B et al (2022) Hydroxy- and amino-phosphonates and -bisphosphonates: synthetic methods and their biological applications. Front Chem 10:890696
17. Liu W et al (2018) Alpl prevents bone ageing sensitivity by specifically regulating senescence and differentiation in mesenchymal stem cells. Bone Res 6:27
18. Nakamura-Takahashi A et al (2020) High-level expression of alkaline phosphatase by adeno-associated virus vector ameliorates pathological bone structure in a hypophosphatasia mouse model. Calcif Tissue Int 106(6):665–677
19. Cheong S et al (2014) Bisphosphonate uptake in areas of tooth extraction or periapical disease. J Oral Maxillofac Surg 72(12):2461–2468
20. de Sousa FRN et al (2021) The effect of high concentration of zoledronic acid on tooth induced movement and its repercussion on root, periodontal ligament and alveolar bone tissues in rats. Sci Rep 11(1):7672
21. Mizutani K et al (2020) Inflammatory skin-derived cytokines accelerate osteoporosis in mice with persistent skin inflammation. Int J Mol Sci 21(10):3620
22. Yokoi K et al (2019) Clinical and genetic aspects of mild hypophosphatasia in Japanese patients. Mol Genet Metab Rep 21:100515
23. Zhang J et al (2020) Interaction between C/EBPβ and RUNX2 promotes apoptosis of chondrocytes during human lumbar facet joint degeneration. J Mol Histol 51(4):401–410
24. Zhang M et al (2021) Xanthohumol attenuated inflammation and ECM degradation by mediating HO-1/C/EBPβ pathway in osteoarthritis chondrocytes. Front Pharmacol 12:680585
25. Koelling S et al (2006) Cartilage oligomeric matrix protein is involved in human limb development and in the pathogenesis of osteoarthritis. Arthritis Res Ther 8(3):R56
26. Cui J, Zhang J (2022) Cartilage oligomeric matrix protein, diseases, and therapeutic opportunities. Int J Mol Sci 23(16):9253
27. Mizoguchi I et al (1997) Localization of types I, II and X collagen and osteocalcin in intramembranous, endochondral and chondroid bone of rats. Anat Embryol (Berl) 196(4):291–297

28. Paul S et al (2016) Ihha induces hybrid cartilage-bone cells during zebrafish jawbone regeneration. Development 143(12):2066–2076
29. Kushioka J et al (2020) A novel negative regulatory mechanism of Smurf2 in BMP/Smad signaling in bone. Bone Res 8(1):41
30. Xu Z et al (2017) SMURF2 regulates bone homeostasis by disrupting SMAD3 interaction with vitamin D receptor in osteoblasts. Nat Commun 8:14570
31. Michigami T et al (2020) Clinical practice guidelines for hypophosphatasia. Clin Pediatr Endocrinol 29(1):9–24
32. Vinan-Vega MN, Abate EG (2018) Hypophosphatasia: clinical assessment and management in the adult patient-a narrative review. Endocr Pract 24(12):1086–1092
33. Yamauchi M, Sugimoto T (2015) On "2015 guidelines for prevention and treatment of osteoporosis". Medical treatment for osteoporosis. Clin Calcium 25(9):1285–1292
34. Bessueille L et al (2020) Tissue-nonspecific alkaline phosphatase is an anti-inflammatory nucleotidase. Bone 133:115262